Design and optimization of Bandwidth Part selection for massive beamforming

Juan Guirado López-Puigcerver
ju4288gu-s@student.lu.se

Department of Electrical and Information Technology
Lund University

Supervisors: Harish Venkatraman (Ericsson)
Ove Edfors(EIT)

Examiner: Fredrik Rusek

June 26, 2020

Printed in Sweden
Tryckeriet i E-huset, Lund

The present is theirs; the future, for which I really worked, is mine.
— Nikola Tesla

First, I would like to dedicate this Master thesis to my parents. Thank you, Dad, for being my mentor throughout my college years and for always advising me so well. Thank you also, Mom, for having always supported me and listened to me whenever I needed help.

Then, I would like to thank Ericsson, especially to Mladen Toncev and Harish Venkatraman, for the opportunity of carrying out this Master Thesis and for all the support.

Finally, I want to also mention all my family and friends for being there whenever I needed it. I dedicate this thesis to my family in Madrid and Almeria, to friends from Cobeña and surroundings, to my friends from the ETSIT UPM, and to my partners of adventures in Lund. Thanks for everything.

Juan Guirado

Abstract

In the last 30 years, a new mobile communications generation has been developed every 7 to 10 years. The last one that is currently under development is the Fifth Generation. This generation aims to fulfill a wide range of requirements for different use cases. To that end, a new radio access technology called New Radio (NR) has been developed.

The main design principle behind NR is to allow enough flexibility to meet all the new requirements. This flexibility is, for instance, reflected in the use of the spectrum, where the concept of Bandwidth Part (BWP) was created. NR supports a large bandwidth in comparison to previous generations. However, not all the User Equipment (UEs) can manage such large bandwidth. As a consequence, the concept of BWPs was introduced.

By using BWPs, the carrier can be subdivided and used for different purposes, although the use of BWPs might affect other NR features, such as beamforming. Thus, the impact of BWPs in MU-MIMO grouping had to be analyzed. However, the bandwidth parts also create an opportunity to optimize the use of MU-MIMO grouping concurrently with BWPs. For that reason, we developed a BWP selection algorithm in this project that is able to respond to the beamforming degradation.

In order to develop that algorithm, a simulator following the specifications of the 3GPP was designed and implemented in MATLAB. As beamforming was one of the cornerstones of the project, a realistic channel model with spatial consistency was needed. We selected WINNER II for the channel model.

Then, the BWP selection algorithm, which based on the Direction of Arrival for selecting the optimal MU-MIMO grouping, was developed. The results of the simulations show that the algorithm optimizes the Bit Error Rate performance when the beamforming is degraded.

Keywords

Mobile communications, 5G, New Radio (NR), Bandwidth Part (BWP), Beamforming, MU-MIMO

Popular Science Summary

Optimizing the coexistence of the new mobile generation (5G) features called bandwidth part and beamforming

The new mobile communications generation (5G) brings many new advanced features to meet the new arising requirements. Bandwidth Parts and massive beamforming are some examples. This project optimized the interoperability of those two features.

The Fifth mobile communications generation is the latest being developed after 30 years of evolution of mobile technologies. The world is experiencing a great digital transformation that is changing society in many aspects, such as economy, culture, education, or even social relationships. Inside this revolution, mobile communication technologies are playing a significant role.

Around every 7 to 10 years, a new mobile generation, e.g., 3G, 4G or 5G, has appeared bringing more advanced features, such as a fastest access to the Internet. For the user, this is usually translated in new functionalities in their devices or higher-quality access to media like videos or conferences.

One of the reasons why mobile communications can evolve so quickly and in sync around the world is standardization. Standardization allows the industry to jointly develop new generations of mobile telephony in a global effort so that all devices are compatible. In other words, users of terminals from different manufacturers can communicate with each other. The international body in charge of the standardization of mobile communication generations is the 3GPP.

Since 2012, the 3GPP is focused on the standardization of the Fifth Generation (5G). The main feature of this new generation is that it aims to fulfill new use cases divided into three groups. In a few words, the new requirements are to enable even more extensive data volumes and enhanced user experience, connect a massive number of machine devices to the Internet and offer services with high reliability or timing requirements such as telemedicine.

Because of this broad range of use cases, the main design principle of the new generation standard is to allow enough flexibility to meet all the requirements given by the use cases. As a consequence, the new standard introduces a new concept called Bandwidth Parts (BWP). Bandwith Part is a new concept that allows flexibility in the use of the electromagnetic spectrum.

However, the introduction of this new feature might impact other techniques that were already introduced in mobile communications, such as beamforming. Beamforming is a technique that allows more efficient use of the resources to obtain higher data-rates in the system.

For that reason, this project researched the interoperability of those techniques looking to optimize the use of both features. To that end, a simulator was developed, emulating a real-world environment. The results show that it is feasible to improve the system capacity if both parameters are considered together. As a consequence, a system capacity improvement can be translated into a better user experience.

Table of Contents

List of Figures

List of Tables

Chapter 1

Introduction and objectives

1.1 Introduction

Mobile communications never stop evolving. Although Long-Term Evolution (LTE) has become the most successful wireless broadband technology across the world, new arising requirements make it necessary to create and standardize a new radio access for the next generation (5G). This new radio access is known as New Radio (NR).

One of the main challenges of 5G is to support a high data rate. For that reason, a large bandwidth (100 MHz) has been proposed in NR. However, transmitting/receiving signals with such a large bandwidth all the time is not convenient from a power consumption point of view. In order to solve that problem, the concept of Bandwidth Part (BWP) was introduced in NR.

The bandwidth parts allow the receivers to use bandwidth adaptation so that they can use a narrow bandwidth for monitoring control channels and a wider one for sending large amounts of data. One BWP is characterized by a certain numerology (OFDM subcarrier spacing) and a set of consecutive resource blocks (set of NR subcarriers).

Although the use of bandwidth parts solves the problem of supporting large bandwidth, it might impact the performance of an NR radio access network. In particular, the bandwidth parts might affect the massive beamforming and MU-MIMO (Multiple-User MIMO) grouping. However, it also creates an opportunity to optimize the use of MU-MIMO grouping concurrently with the use of bandwidth parts. Consequently, a detailed analysis of using Bandwidth Parts, together with massive beamforming, is needed.

This project was carried out with the collaboration and supervision of Ericsson AB, one of the world's leading information and communication technology companies and one of the main companies developing 5G networks.

1.2 Objectives and contributions

The main goal of this project was to find and design a solution that optimizes the BWP selection from a network performance point of view when MU-MIMO

grouping is used. The aim is to optimize the selection of BWPs and MU-MIMO grouping together in order to maximize the cell capacity.

To that end, an NR simulator was designed and implemented in MATLAB, in which a BWP allocation could be done and changed dynamically with the temporal evolution of the simulation.

In addition, one selection algorithm was developed, reaching a cell capacity improvement when the users move in an environment so that the beamforming is impacted. This simulator follows the Specifications of the 3GPP for 5G/NR. Thus, the results are a proof of concept applicable to the real world.

1.3 State of the art

One of the challenges of this Master thesis was to find related work in this field because 5G/NR is a new technology that is still being standardized. For that reason, there is a lack of previous studies, and the NR specifications are still under review. Bandwidth Parts were introduced in Release 15 of the 3GPP [1], and specified in the Technical Specification 38.211 [2].

Then, there are not many publications about the optimization of BWP switching or selection. Abinader et al. published a study about the impact of Bandwidth Part Switching on 5G NR System Performance in 2019 [3]. However, the goal of this research was to analyze the impact of BWP switching due to the switching timers and delays. Thus, the study is done in higher layers than this thesis, and the focus is the system latency and delay. As a consequence, the results can not be applied to this thesis, although it motivates more the analysis of BWP switching impact in the Physical Layer.

Finally, the development of a simulator to test the BWP switching algorithms needs a study of the most realistic channel models that can be applied to validate the algorithms. The 3GPP developed a study on channel model from frequencies from 0.5 GHz to 100 GHz [4] that includes the state of the art of channel modeling for high frequencies. Apart from this compilation of work outside the 3GPP, this technical report also includes one channel model developed by the 3GPP. Besides, Shihao Ju et al. published in 2018 one paper that included the main spatial consistent channel models [5]. Spatial consistency is one desired feature for the channel models when beamforming is simulated 3.8. Finally, Fjollla Ademaj et al. presented in A Spatial Consistency Model for Geometry-Based Stochastic Channels [6] a survey on existing channel models and how they can be classified.

1.4 Structure of the report

This report is organized as follows: Chapter 2 presents the background of 5G and NR, including the road to 5G, the novelties of 5G, and the use cases. Then, in Chapter 3, the technical characteristics of NR are explained, as well as the channel modeling for NR. Chapter 4 introduces the design and implementation of the simulator, with all the characteristics and design principles. After, the BWP selec-

tion algorithm is developed in chapter 5. In chapter 6, the results of the Master Thesis research are presented, and finally, chapter 7 concludes the report.

Chapter 2

Background: 5G and NR

2.1 The road to the Fifth Generation

Since the emerge of the first generation of mobile communications (1980), the world has witnessed a new generation every 7 to 10 years. Each generation is designed to serve the social needs over 2 to 3 decades [7].

The first generation was based on analog transmission and was limited to voice services. Different analog technologies were developed in each country, from which stand out AMPS (Advanced Mobile Phone System), in North America, or NMT (Nordisk MobilTelefoni) in the Nordic countries. The second generation emerged in the early 1990s, and it introduced the digital transmission on the radio link. Although different technologies were created, GSM outstands because of being developed jointly by many European countries. Besides, despite being focused on voice services, this generation also provided limited data services.

In early 2000, the third generation was introduced. This generation was the result of a real global standardization when, in 1998, the different regional standardization organizations joined and created the Third-Generation Partnership Project (3GPP). The 3G brought high-quality mobile broadband that enabled fast wireless access to Internet data, especially when the 3G evolution, called HSPA (High-Speed Packet Access) came. The radio access in this generation was based in CDMA modulation, and also introduced Time Division Duplex (TDD), which is one of the foundations of this Master Thesis.

The last generation that has been largely deployed is the Fourth Generation, which is represented by the LTE technology. Following the path of the third generation, the 4G was also standardized by the 3GPP. This technology is based on OFDM transmission enabling wider bandwidths and more advanced multi-antenna technologies. Besides, it supports FDD and TDD operations.

As with the second or third generation, LTE evolved inside the third generation. In fact, the first release of LTE in 2008 (Rel. 8) did not meet the 4G technical criteria. This evolution was carried through new 3GPP releases so that the performance was enhanced, and the capabilities extended. Consequently, this evolution allowed higher end-user rates and higher spectrum efficiency. Along with this evolution of LTE, the Fifth Generation began to be discussed in 2012, starting

with the use cases. Some of these use cases can be fulfilled with the latest evolutions of LTE. Because of that, LTE should be seen as an essential part of the 5G radio-access solution, although it is not a new standardized technology for the Fifth Generation [8].

However, some requirements can not be met with LTE or its evolution. As a consequence, a new radio access technology started to be developed by the 3GPP. It is known as NR (New Radio).

2.2 The Next Generation: 5G/NR

As stated before, the discussions on the Fifth Generation started around 2012. However, 3GPP began the work on the specification of 5G in March 2017 [7].

The standardization work was divided into two phases: the standardization of the fundamental building blocks (Release 15) and further enhancements (Release 16). Fig. 2.1 shows the timeline of those distributions.

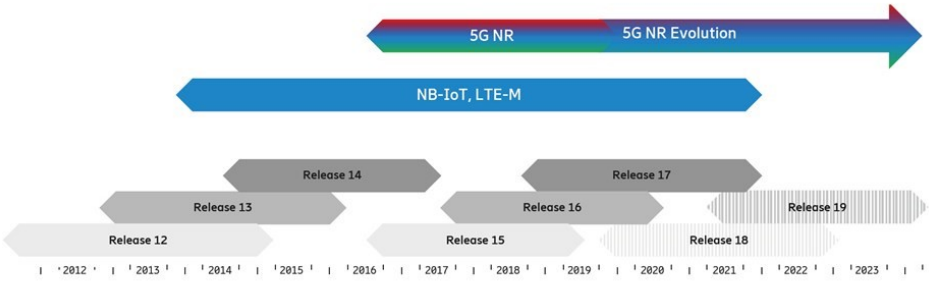

Figure 2.1: 3GPP Releases evolution.

Source: Ericsson [7]

Although the new Radio Access technology in 5G is NR, to accelerate the 5G implementation process, LTE was also considered in Release 15. Thus, Release 15 was divided into three steps. The first step was called Non-standalone (NSA) and was completed in December 2017. In this step, the Evolved Packet Core (EPC) from LTE is essential for initial access and user mobility. The second step is the standalone (SA) mode, which was finished in June 2017 and in which NR is independent of LTE. Finally, there was a third step finished in March 2019 with other architecture options.

Many times, the term 5G is used to refer to the new 5G radio access technology. However, it is a much general concept that includes a wide range of new services envisioned in the future of mobile communications. Therefore, it is essential to talk about use cases.

2.2.1 Use cases

The range of use cases considered in the standardization process of 5G is extensive. For instance, the Next Generation Mobile Networks (NGMN) Alliance developed twenty-five use cases for 5G in their white paper from 2015 [9]. They grouped those use cases into eight families. However, the 5G use cases are most commonly organized into three classes: enhanced mobile broadband (eMBB), massive machine-type communications (mMTC), and ultra-reliable low latency communications (URLLC). See Fig. 2.2.

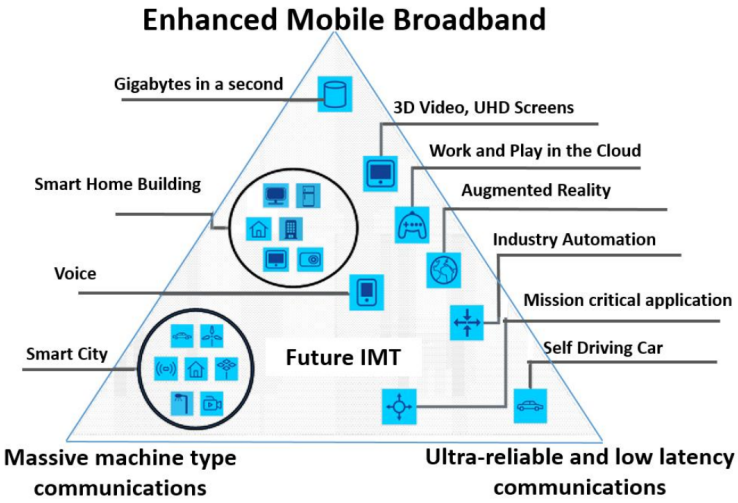

Figure 2.2: 5G Use Cases.

Source: ITU

Enhanced mobile broadband is a more or less straightforward evolution of the mobile broadband services provided to us today. The main goal is to enable even larger data volumes and enhanced user experience.

The main focus of massive machine-type communications is on providing connectivity to a massive number of devices, such as remote sensors or actuators. In essence, these devices have low complexity, low battery consumption, use a narrow bandwidth, and send (or receive) small amounts of data.

Finally, the ultra-reliable low latency communications services are those with stringent requirements on reliability and latency, like autonomous vehicles, automatic control or Augmented Reality and Virtual Reality (AR/VR).

2.2.2 Main changes and New features

Although NR uses many of the structures and features of LTE, the 3GPP decided that this new access radio was needed to meet the requirements of the 5G use cases. The main reason to develop a new access radio instead of evolving LTE was that backward compatibility is not required.

Thus, the main focus on the design of NR was to enable forward compatibility to future enhancements so that the requirements for all the use cases can be fulfilled. Thus, flexibility in the use of the resources is desired so that different configurations are possible to meet the different requirements. In addition to this design principle, we can also highlight, higher frequency operation and spectrum flexibility, ultra-lean design, low latency and high reliability, and beam-centric design [8].

One of the main features of NR is that it will be deployed in new frequency bands, operating in low frequencies below 1 GHz up to frequencies around 60 GHz. We can distinguish three parts of the spectrum that are being exploited: low-band, below 2.5 GHz; mid-band in the range of 2.5-10 GHz, and high-band, the so-called mm-waves above 24 GHz [7]. However, the 3GPP divides the operating frequency bands for NR only in two frequency ranges: FR1 (410 MHz – 7125 MHz) and FR2 (24250 MHz – 52600 MHz) [10], [11].

The ultra-lean design principle consists of minimizing the always-on transmissions, i.e., transmissions carried by network nodes regardless of the amount of user traffic. This way, energy performance is improved, and higher data rates can be achieved. In fact, this principle is highly related to the forward compatibility goal, as always-on signals occupy resources and impose restrictions on future developments.

The low latency support has also impacted many details of the NR design. For instance, it influenced the design of the reference signals and control signaling, as well as high-order protocols such as Medium Access Control (MAC) or Radio Link Control (RLC).

Finally, 3GPP is also developing a new 5G core network that is called 5GCN, which is built upon the EPC with three new areas of enhancements: service-based architecture, support for network slicing, and control-plane/user-plane split.

Chapter 3

NR Overview: Technical characteristics

In this chapter, the main technical characteristics and specifications of the NR physical layer that are relevant for this project are introduced. We are namely focused on the Physical Layer because upper layers are not directly relevant for this project. Then, a discussion about channel modeling for simulations is added at the end of this chapter.

3.1 Transmission Structure

In general, the NR architecture is based on the architecture of LTE but redesigned to omit always-in signals (ultra-lean principle) and adding more flexibility (forward compatibility). For instance, NR uses OFDM for the downlink waveform, and so did LTE. Nevertheless, it differs from LTE, where DFT-precoded OFDM was the only scheme while in NR, it is only optional.

The motivation for using DFT-precoded was to reduce the PAPR (Peak-to-Average Power Ratio) in the User Equipment (UE) so that high power-amplifier efficiency is achieved. However, NR prioritizes the desire to have the same transmission scheme in both uplink and downlink while having simpler receiver structures that are more appropriate for spatial multiplexing. Having the same transmission scheme for the uplink and downlink is desired to enable future enhancements such as sidelinks, i.e., transmissions between UEs. Besides, DFT-precoding also imposes scheduling restrictions, as only contiguous allocations in the frequency domain are possible.

One of the main novelties of NR over LTE is that NR does not impose a certain subcarrier spacing and cyclic prefix length in OFDM, i.e., the numerology. The numerology is an important selection in OFDM because it has to be a compromise between resistance to frequency errors and phase noise (large spacing), and resistance to Doppler spread/shift (short spacing and, thus, short cyclic period).

LTE fixed the subcarrier spacing at 15 kHz and the cyclic prefix at 4.7 µs., which was a good selection for the scenarios for which LTE was designed. However, NR is designed to support a wide range of deployment scenarios. Thus,

having a single numerology for NR is not an option. The engineers decided then to allow flexibility to the selection of the numerology, with even having different ones in the same cell. Nevertheless, the possible numerologies were restricted to scalings by powers of 2 of the 15 kHz numerology. The reason was to allow compatibility with LTE, especially for the eMTC devices that work with LTE.

The possible numerologies are gathered up in Table 3.1 [2]. As we can see, the minimum carrier spacing is 15 kHz, and the maximum one is 240 kHz. However, not all the numerologies are supported for all the frequency bands, even though NR physical-layer specifications are band agnostic. Table 3.1 also shows the numerologies in which each subcarrier spacing is supported [10], [11]. Note that 240 kHz is only supported for the SS block.

μ	**Subcarrier Spacing (kHz)**	**Cyclic Prefix (μs)**	**Frequency Range**
0	15	4.7	FR1
1	30	2.3	FR1
2	60	1.2	FR1 and FR2
3	120	0.59	FR2
4	240	0.29	-

Table 3.1: Supported transmission numerologies

Finally, LTE also defines two different cyclic prefix sizes: normal and extended. The extended was created for big cells where the time dispersion impacted the performance. However, it was not used in practical deployments. For that reason, NR has only kept it for the 60 kHz subcarrier spacing numerology.

3.1.1 Time-domain structure

NR is organized in time-domain into frames of 10 ms duration. Those frames are also divided into 10 subframes with 1 ms duration. Then, the subframe is divided into slots (this number depends on the numerology), which are composed of 14 OFDM symbols. However, if the extended cycled prefix is used, then a slot is only composed of 12 OFDM symbols [2]. Table 3.2 presents the number of OFDM symbols per slot, slots per frame, and slots per subframe.

Thus, for the first numerology (15 kHz of carrier spacing), an NR slot has the same structure as an LTE subframe with a normal cyclic prefix, which was desired for the reasons stated in the previous section. Another important characteristic of NR supports occupying only a part of the slot, which is called "mini-slot transmission." This characteristic is beneficial for low latency or operation in unlicensed spectra.

3.1.2 Frequency-domain Structure

The smallest physical resource in NR is a resource element, which consists of one subcarrier during one OFDM symbol. Twelve consecutive subcarriers form one resource block. Note that the resource block is a one-dimensional measure which

μ	OFDM Symbols per slot	Slots per frame	Slots per subframe
0	14	10	1
1	14	20	2
2	14	40	4
2^{ext}	12	40	4
3	14	80	8
4	14	160	16

Table 3.2: Frames, subframes, slots and OFDM symbols per numerology

Source: Inspired by [2]

is only defined for the frequency domain. It should not be confused with an LTE Resource Block.

Due to the different numerologies supported by NR, a resource block does not have a defined bandwidth. Instead, the bandwidth depends on the numerology, although the boundaries are synchronized. For instance, one resource block with a subcarrier separation of 30 kHz occupies the double than one with a subcarrier separation of 15 kHz.

Another essential feature of NR is that the devices do not have to support the full carrier bandwidth. In LTE, the carrier bandwidth was fixed to 20 MHz, and all the devices had to support that bandwidth. However, NR is designed to support bandwidths up to 400 MHz, although it is not reasonable to impose the user terminals to support that bandwidth. For that reason, that requirement was withdrawn. However, this also implies some challenges from the DC (central subcarrier) management point of view, and for the initial access. These challenges are out of the scope of this thesis but can be consulted in [8].

3.2 Channels in NR

There are three levels of channels in NR: logical, transport and physical channels. They are organized hierarchically so that logical channels are mapped into transport channels and transport channels into physical channels (see Fig 3.1).

The logical channels provide MAC services to the Radio-Link Control Protocol (RLC). These channels are defined by the information that they carry. There are two types of logical channels: traffic and control channels. The only traffic channel is the Dedicated Traffic Channel (DTCH). The control channels are the Broadcast Control Channel (BCCH), the Paging Control Channel (PCCH), the Common Control Channel (CCCH) and the Dedicated Control Channel (DCCH).

The transport channels are defined by how and with what characteristics the information s transmitted over the radio interface [8]. There are five transport channels: the Broadcast Channel (BCH), the Paging Channel (PCH), the Downlink Shared Channel (DL-SCH), the Uplink Shared Channel (UL-SCH) and the

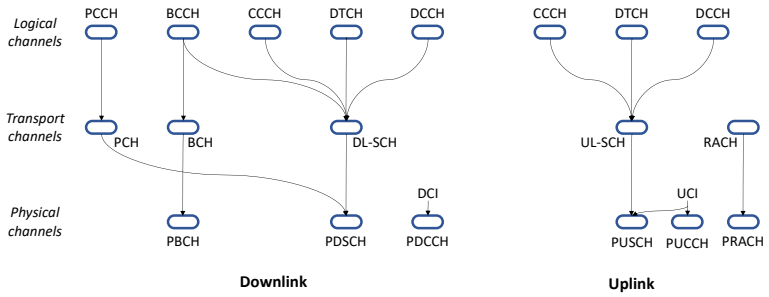

Figure 3.1: NR Channels.

Random-Access Channel (RACH). The latter does not carry any transport block, but it is used for the initial access.

Finally, the physical channels, which are the only ones considered in this thesis, correspond to the set of time-frequency resources used for transmission of a particular transport channel. The physical channels are Physical Downlink Shared Channel (PDSCH), Physical Downlink Control Channel (PDCCH), Physical Uplink Shared Channel (PUSCH), Physical Uplink Control Channel (PUCCH), Physical Broadcast Channel (PBCH) and Physical Random-Access Channel (PRACH). In this thesis, only the PDSCH and the PUSCH are considered, which are the ones that carry the user data.

3.3 Data transmission Block Chain

The processing chain in NR is not the same for all the channels. In this section, we introduce the processing chain for the channels that are used in this project: PDSCH and PUSCH. Besides, the transport channel processing chains, which include, for instance, Code Redundancy Check (CRC) or channel coding, are not considered as they don't impact the results of this project.

The PDSCH and PUSCH block chains are, in general, very similar, and they only differ in some features [12].

3.3.1 PDSCH processing chain

The input of the chain is the corresponding transport channel, i.e., DL-SCH, where the CRC and coding were added to the information.

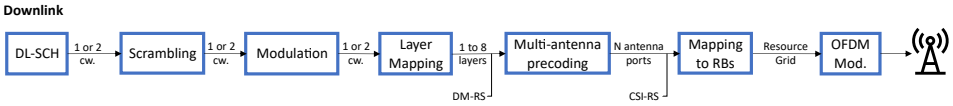

Figure 3.2: PDSCH processing chain.

Then, the first block is the scrambling, which is used to ensure full utilization

of the processing gain provided by channel coding, as it randomizes the interfering signals.

The second block is the modulation. This module transforms the block of scrambled bits into a block of complex symbols. The modulation schemes supported by the PDSCH channel are QPSK, 16QAM, 64QAM, and 256QAM.

The layer mapping step is intended to distribute the modulated symbol across the different transmission layers. This layer mapping is done so that each nth symbol is mapped to the nth layer. One codeword can be mapped to up to four layers. As two codewords can be supported in the downlink, the PDSCH channel supports up to eight layers.

The multi-antenna precoding maps the transmission layers to a set of antenna ports using a precoder matrix. This block is the one that achieves beamforming and spatial multiplexing. More details are given in Sec. 3.7.

Then, the resource mapping block maps the modulation symbols to be transmitted in each antenna port and maps them to the set of available resource elements assigned by the MAC scheduler.

Finally, the OFDM modulation is carried out to obtain the signal to be transmitted.

3.3.2 PUSCH processing chain

The uplink processing chain of the PUSCH is very similar to the one of the PDSCH. Thus, only the main differences are discussed in this section.

Figure 3.3: PUSCH processing chain.

First, the input of the PUSCH processing chain is the transport channel UL-SCH. There are no big differences to be commented about the scrambling block.

Then, the PUSCH supports the same modulations as the PDSCH plus $\pi/2$-BPSK, which can only be used if transform precoding is also used.

The layer mapping block only allows up to four layers for the uplink, as in the uplink, only one codeword is supported. Besides, if transform precoding is used, only one layer can be used.

The multi-antenna precoding also differs from the downlink, namely in the way the beamforming is selected, but, again, more information is given in Sec. 3.7.

Finally, the resource mapping and the OFDM modulation blocks work very similarly to the ones in the downlink.

3.4 Bandwidth Parts

The bandwidth part is a new concept that appears in NR to enable more flexibility to the assignment of resources in a given carrier. As stated in sec. 3.1.2, NR supports large bandwidths in comparison with LTE. These bandwidths can be supported by base stations, but not by every terminal, as that would be, among other drawbacks, costly in terms of device energy consumption. That is the origin of the Bandwidth Part (BWP).

This way, the carrier can be subdivided and used for different purposes. A Bandwidth Part is characterized by a numerology and a set of consecutive resource blocks. Thus, each BWP can be configured differently so that signals with different requirements can be integrated.

A UE can be configured up to four BWPs in the uplink and up to four BWPs in the downlink. In the case of a supplementary uplink, four additional BWPs can be configured [13]. However, only one BWP for the uplink and one for the downlink can be activated at a given time. This means that a device is not assumed to be able to transmit or receive outside the bandwidth part.

The gNB activates and deactivates the BWPs of a UE using the same downlink control signaling as for scheduling information, achieving a fast switching between BWPs.

3.5 Duplex Scheme

Following the flexibility principle of NR again, it supports the separation of uplink and downlink in time and/or frequency domain, using the same frame structure. Thus, NR supports TDD and FDD.

In TDD, the uplink and the downlink use the same carrier frequency, and they are separated in time. Besides, NR supports dynamic TDD. In this scheme, the slots (or parts of the slots) can be dynamically allocated to either the uplink or the downlink. Thus, the provision can be adjusted to the requirements at a given time.

In FDD, the uplink and the downlink use different carrier frequencies, so they are separated in frequency. If the transmission of the uplink and the downlink are carried out at the same time, then we talk about the full-duplex. However, if those transmissions are also separated in the time domain, the operation mode is half-duplex FDD.

In this thesis, we consider all the time that the operation mode is TDD, which enables us to make channel estimations for the downlink using reference signals from the uplink. This is called channel reciprocity.

3.6 Channel Sounding

Most of the complex techniques used nowadays in modern mobile communications are based on the availability of more or less detailed knowledge about the

channel characteristics. Thus, estimating the channel is essential for applying these techniques.

This channel estimation can be performed in different ways. In this project, we take advantage of channel reciprocity, assuming that channel characteristics are equivalent to the uplink and downlink. This allows us to sound the uplink channel to acquire information about the channel that is used for the downlink.

In order to obtain that information, reference signals are used. In NR, the reference signals for uplink sounding are called *Sounding Reference Signals* (SRS). This signal is the uplink equivalent to the downlink CSI-RS. However, as the SRS is an uplink signal, it was designed to have low cubic-metric (PAPR), enabling high device power-amplifier efficiency.

The time-frequency structure of an SRS has a *comb* structure and can occupy one, two, or more OFDM symbols at the end of a slot. In the frequency domain, the SRS for one user is transmitted every Nth subcarrier, where N is two or four. This way, the SRS for more than one user can be frequency multiplexed.

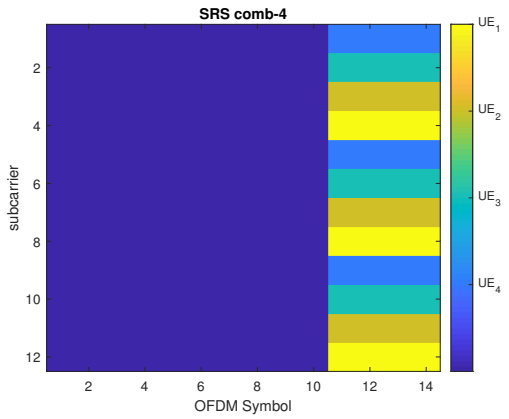

Figure 3.4: SRS time-frequency structure.

In order to achieve low cubic-metric, the SRS is based on the *Zadoff-Chu* sequences [2]. These sequences are given by Expression 3.1 for a given length M:

$$z_i^u = e^{-j\frac{\pi u i(i+1)}{M}}; \quad 0 \leq i < M \tag{3.1}$$

The key property of the Zadoff-Chu sequences is that the Fourier transform of these sequences is another Zadoff-Chu sequence. Thus, a constant time-domain amplitude implies a flat spectrum. In addition, they have the property that two different time-domain cyclic shifts of the same sequence are orthogonal to each other.

Finally, if an SRS has to support more than one antenna port, the ports share the same set of resource elements and the same SRS sequence, but a phase rotation in the frequency domain is applied to obtain orthogonal sequences.

3.7 MU-MIMO: Beamforming

One of the key features of NR, which was already also introduced in LTE, is the multi-antenna transmission. There are several benefits of using multiple antennas in a mobile communication system, such as array gain, diversity gain, spatial multiplexing, and interference reduction [14]. In this project, multi-antenna transmission is used for beamforming and Multiple User MIMO (MU-MIMO). Beamforming consists of using the channel information to focus energy in a particular direction. This way, array gain and interference reduction are achieved. MU-MIMO consists of achieving spatial multiplexing for different users so that they can use the same time-frequency resources concurrently. An MU-MIMO group is a set of users that use this time-frequency resources concurrently.

Beamforming and MU-MIMO grouping are the cornerstones of this project, as we want to evaluate the impact of the BWPs on this beamforming, i.e., see how to optimize the interaction of these two concepts in the system.

Different beamforming techniques can be applied. In this project, we implemented three of them, that are introduced in this section, but first, a mathematical model of the beamforming is presented.

The basic MIMO system equation is usually represented as

$$\boldsymbol{y} = \boldsymbol{H_{DL}}\boldsymbol{x} + \boldsymbol{n} \tag{3.2}$$

Where $\boldsymbol{x}$ is the transmitted signal with size (N_{Tx} x 1), where N_{Tx} is the number of transmitting antennas; $\boldsymbol{n}$ is the noise vector (N_{Rx} x 1), and $\boldsymbol{y}$ is the received signal (N_{Rx} x 1). We are considering here the simple case in which N_{Rx} is equal to the number of users, i.e., the users only have one antenna. This has been the assumption in this project for obtaining the results, although the simulator allows more than one antenna per UE.

Then, beamforming consists in multiplying the transmitted signal by a weighting matrix $\boldsymbol{W}$, so that

$$\boldsymbol{x} = \sqrt{P_{Tx}}\boldsymbol{W}\boldsymbol{x} \tag{3.3}$$

In order to mantain the downlink available power, the weighting matrix is normalized with equal transmit power for all the UEs.

Where P_{Tx} is the base station transmitted power. Then, three strategies for computing the weighting matrix are presented

3.7.1 Maximum Ratio Transmission

This technique, also known as match filter, maximizes the SNR for each user. For that purpose, the weighting matrix is computed as the complex conjugate of the channel matrix.

$$\boldsymbol{W} = \boldsymbol{H}^H \tag{3.4}$$

The complexity of the computations is low. However, this technique is very sensitive to user interference.

3.7.2 Zero-Forcing

This algorithm maximizes the signal to interference and noise ratio (SINR). In this case, the weighting matrix is given by the pseudo-inverse of the channel matrix.

$$\boldsymbol{W} = \boldsymbol{H}^H \left(\boldsymbol{H}\boldsymbol{H}^H \right)^{-1} \tag{3.5}$$

This algorithm can cancel the interference between users. However, the complexity of the algorithm is higher.

3.7.3 Regularized Zero-Forcing

This version of the Zero-Forcing algorithm adds the noise variance to reduce the effect of the noise in the system. It is also known as the MMSE algorithm. If the SNR is very high, this algorithm converges to the MRT. However, if the SNR is very low, the algorithm converges to the ZF.

$$\boldsymbol{W} = \boldsymbol{H}^H \left(\boldsymbol{H}\boldsymbol{H}^H + \alpha \boldsymbol{I} \right)^{-1} \tag{3.6}$$

Where $\alpha = \frac{K\omega_n^2}{P_d}$, K is a constant, ω_n^2 is the noise variance and P_d is the downlink power.

3.8 Channel modeling

When evaluating the fulfillment of the 5G requirements in an NR system, an essential step is to simulate. Simulations allow us to validate the products and change them easily in a controlled environment before testing in the real world. It is crucial to have a realistic channel model to make these simulations possible so that they emulate all the characteristics of the environment. Standardization bodies such as the 3GPP also carry out studies about the channel models and propose some of them in their technical reports. For instance, the 3GPP developed a channel model for 5G [4]. Also, other modeling works outside the 3GPP are gathered in this reference.

MIMO channel models can be classified into two broad categories: analytical and physical models [15]. The analytical models do not consider the wave propagation models but mathematically describe the channel. Some examples are independent and identically distributed (i.i.d.) channels or the Kronecker Model. Then, the physical models describe the channel based on the electromagnetic properties of the environment.

The physical channel models can further be divided into three categories: deterministic, geometry-based stochastic, and stochastic models [6]. In the deterministic channels, the physical channel parameters, like angular profile or power delay profile, depend entirely on the geometry of the environment. However, in the stochastic models, those parameters are determined in an entirely stochastic way. Finally, the geometric-based stochastic models are in-between. This means

that the location of the scatters is not explicitly specified. Instead, the multipath is characterized by delay, power and direction of the rays. Those parameters are computed from a random scattering environment. Thus, this model allows separating the antenna parameters from propagation parameters, which is convenient for the validation of MIMO systems.

In geometry-based stochastic channel models, we can distinguish between two types of parameters: large-scale parameters (LSPs) and small-scale parameters (SSPs). LSPs are parameters like the root mean square delay spread, the angular spread of departure and arrival, shadow fading and, K-Ricean factor, which change over large distances. If more than one link is established, the correlation of those parameters over the distance has to be considered. This correlation is usually achieved by considering the LSPs as a correlated multivariate random process. Then, the SSPs parameters characterize the multipath components by delay, power, and angular values.

Some examples of geometry-based stochastic channels are the 3GPP-Spatial Channel Model (SCM) [16] or the Wireless World Initiative New Radio (WINNER) [17].

One of the main desired features in geometry-based stochastic channels is spatial consistency or spatial correlation. To reach that, the channel parameters like path loss, LSPs, and SSPs have to show a correlation proportional to the relative distance between the nodes. In essence, if two users are located close, they should experience almost the same channel. This feature is crucial for simulating applications in the context of beamforming. The geometry-based parameters already implement, because of their nature, some kind of consistency. However, the stochastic parameters do not have any relation with the geometry and, thus, show no correlation. As a consequence, the channel behavior is entirely inconsistent, and some kind of correlation has to be added.

For instance, the WINNER II channel [17] already introduces spatial correlation in the LSPs. However, it lacks correlation in the SSPs. The correlation in the SSPs was added following different approaches. For instance, the quasi deterministic radio channel generator (QuaDRiGa) [18] is based on the cluster death-birth process. The COST 2100 channel [19], for example, followed a different approach so that a global set of scatterers is shared by all users through so-called visibility regions.

Chapter 4

Simulation tool: Design and implementation

The main challenge of this project was to design and develop an NR simulator that met all the NR Specifications given by the 3GPP, while being simple and focused on the BWPs evaluation.

As stated in the previous chapter, resource flexibility and ultra-lean design are two of the main characteristics of NR. Because of these principles, designing the simulator with enough flexibility to try different configurations (e.g., numerologies, scenarios, number of resource blocks) was essential for this and further studies on BWPs.

However, the blocks that were identified as not relevant for the study, such as channel coding, were not implemented.

4.1 Design of the simulator

At the beginning of the project, I was provided an LTE simulator as a reference for developing this project [20] [21] [22]. However, we identified that the code didn't have enough flexibility to implement NR characteristics such as BWP, which is the cornerstone of this project, or different numerologies. Besides, the channel model did not meet the desired requirements, namely spatial consistency (see Sec. 4.1.2).

Given that motivation to develop a new simulator from scratch, the design process started. This process can be divided into 4 steps.

1. The needed blocks were identified so that the transmission and receiver chain could be simplified.
2. The characteristics of the channel were analyzed to find a suitable channel model.
3. The simulation procedures were developed so that the BWP selection algorithms could be validated.
4. Design the user-interaction and simulation flow, i.e., which are the steps for the user for configuring and carrying out one simulation.

4.1.1 Block identification

The first step started by identifying which blocks were not needed to implement (see Fig. 4.1).

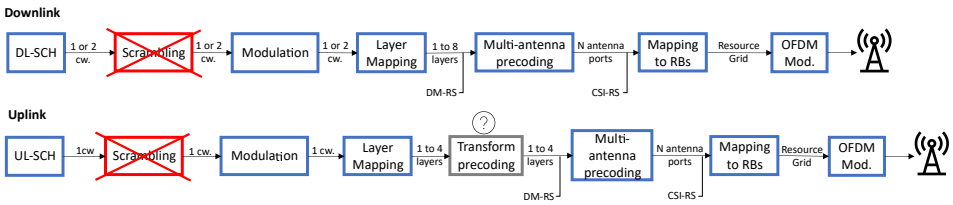

Figure 4.1: PDSCH and PUSCH processing chain with the implemented blocks.

First, the input of the DL-SCH/UL-SCH should be randomly generated in order to obtain good statistical properties for the simulation results. Then, the Scrambling block can be removed, as it does not affect if the stream of bits is already random.

The modulation has to be implemented and should be flexible enough to test different modulation orders.

The layer mapping block is needed if we want to test the transmission of more than one layer, i.e., spatial multiplexing.

The transform precoding block can be left for the uplink, although it is not necessary. Besides, this activation or deactivation of this block can be one of the variables to study.

The multi-antenna precoding is one of the cornerstones of this project, as we want to test the change of BWP when the beamforming performance gets degraded because of the relative position of the users.

Then, the mapping to RBs blocks has to be implemented to allocate the randomly generated bits into the correct resource elements, as the resource grid is also used for sounding reference signals.

Finally, the OFDM block is also essential for the simulation.

4.1.2 Channel model selection

The selection of the channel model is probably the most critical step in the design of this simulator. As stated before, the main goal of the simulator is to test and validate different algorithms for optimal BWP switching. It is essential to choose a channel that shows the closest behavior to reality as possible.

In the beginning, the LTE simulator that I was given implemented fading channels (Rayleigh and Ricean). However, these channels are not appropriate for obtaining the results for this project, as they do not take into account the layout of the simulation scenario. As a consequence, the channel seen by two users that are closely located is not correlated, which does not match what would happen in reality and impacts the results of the simulation. Thus, we needed to find a new appropriate channel model.

For that reason, and following the discussion of Sec. 3.8, the Winner II channel was selected [17]. There were two motivations for selecting such a channel. The first reason was that this channel fulfilled the spatial correlation requirements for this project. Second, and most importantly, because there was a MATLAB implementation developed by MathWorks that could be easily configured and integrated into the code.

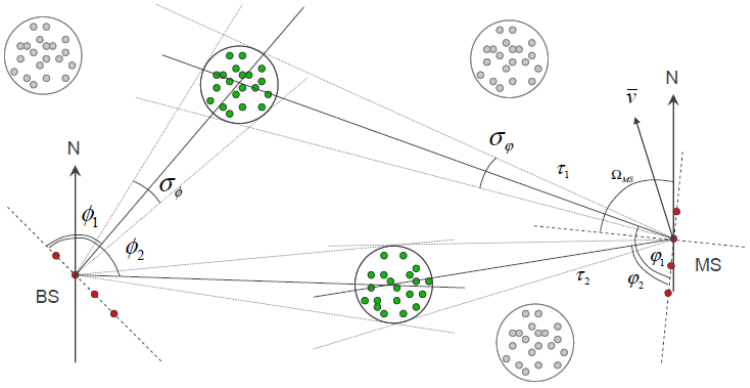

Figure 4.2: WINNER II scatters in a link.

Source: IST [17]

In WINNER II, the channel segments represent a quasi-stationary period during which the change of probability distributions of large-scale parameters can be neglected. Then, this channel model implements spatial consistency by characterizing the transition between segments (cluster death-birth process). Thus, the clusters of "old" segments are replaced by the clusters of "new" segments, and the powers received in the old segments ramp down, and the powers received in the new segments increase [5]. Although there are more advanced techniques for implementing spatial consistency, WINNER II is enough for our project, and it is selected because of being easily integrated into the MATLAB simulator.

4.1.3 Simulation procedures

Once that the main blocks are identified and selected, it is essential to decide how we are going to evaluate the algorithms and which plots we want to show. Once that we know that it is easier to identify over which variables we have to iterate and which variables have to stay constant during the iterations of the simulator.

Two different simulations have been designed for this project. The first one pretends to show the evolution of the performance with the SNR. The second one shows the time-evolution of the UEs moving in the layout so that the BWP switching and the BER performance are presented. In order to explain the simulations, one example is going to be used. In this example, there are two UEs with two different BWP allocation, which at the beginning are 200m separated and at the end of the simulation are just 1 meter one from each other.

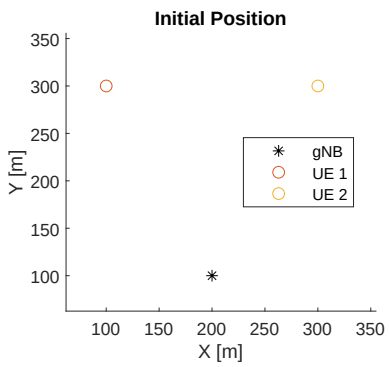

Figure 4.3: Initial position

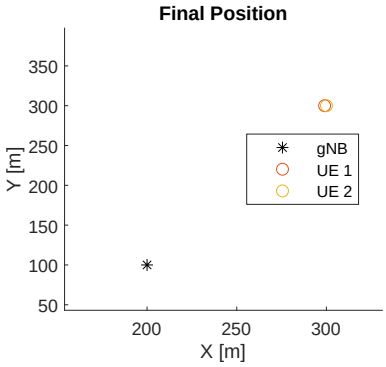

Figure 4.4: Final position

A: SNR-performance

In this simulation, three experiments are run for different SNRs. The first one (Experiment 1) is the initial position, and it is intended as a reference. The UEs are located in some initial positions with an initial BWP allocation that is manually set. Then, the Bit Error Rate (BER) performance is computed for a predefined range of SNRs. For that purpose, first, an uplink subframe is sent. The UEs scheduling is fixed so that every UE gets the same resources for sending reference signals and data. Then, the channel estimation is carried out with the sounding reference signal included in that subframe. As TDD is used in this simulator, this channel estimation can be used for beamforming. Thus, N subframes are sent to the UEs using beamforming. In this case, all the resource elements can be allocated to each UE because of the beamforming. The bit error rate is computed for the uplink and the downlink, although the UL BER is only computed for debugging.

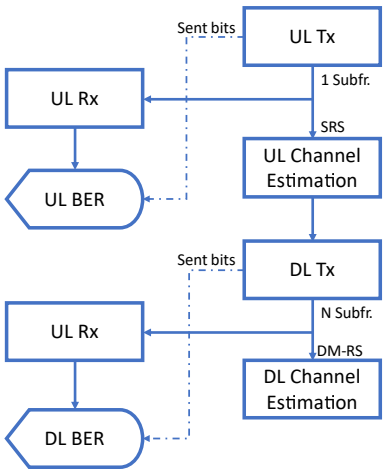

Figure 4.5: Experiment 1 flow.

After the first experiment, the UEs are moved to the desired final positions

in the layout, and two experiments are carried out (Experiments 2 and 3). Experiment 2 follows the same procedure as Experiment 1, but with the new UEs location. The simulation flow of Experiment 3 is a bit different because it introduces the optimization algorithm. This flow is shown in Fig. 4.6.

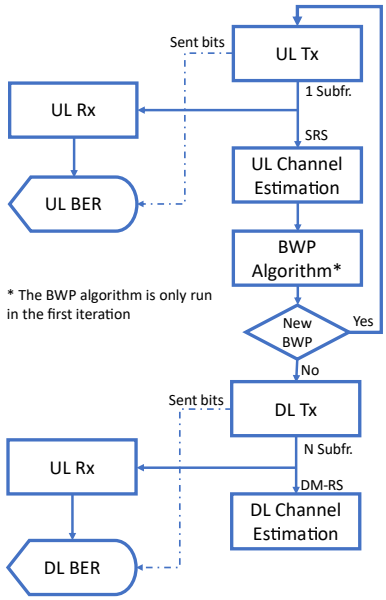

Figure 4.6: Experiment 3 flow.

Once the three experiments are finished, the three BER performances are plot together so that they can be compared.

B: Time performance

This second type of simulation is very similar to the previous one but fixing the SNR. Then, the performance is computed for a given number of snapshots between the initial position and the final position. This way, the evolution of the performance BWP switching algorithm can be seen with respect to the relative position between the UEs.

In this case, only two experiments are executed. The first one follows the same reasoning as Experiment 2 in Simulation A, and the second one follows the same as Experiment 3 in Simulation A. Thus, the two flow diagrams presented for Simulation A also apply for Simulation B.

The main advantage of this simulation is that it allows us to study the behavior of the BWP switching algorithm during all the paths followed by the UEs. Besides, it can also be used for validating the spatial properties of the channel.

4.2 Implementation of the simulator

Once the simulator was designed, the next step was to implement it. We chose MATLAB to implement the simulator because of the broad range of functions that it offers related to signal processing and the easiness to work with signals. Besides, the LTE simulator that I was given was also implemented in MATLAB.

This simulator developed by several students during the past years used MATLAB GUIDE and the LTE toolbox. First, we decided to migrate from GUIDE to MATLAB App Designer [23]. The reason was that MATLAB has decided to remove the GUIDE environment, so in a future release of MATLAB, the GUIDE apps will not be editable. Besides, MATLAB App Designer offers some features that make the apps more dynamic and responsive to the screen size. Also, the GUI objects (e.g., buttons, texts...) are easier to handle.

Second, the LTE Toolbox had also to be substituted. The main reason was that it does not support NR features like BWPs, which were critical for this project. Besides, the 5G NR Toolbox could not be used because of license issues, so all the functions had to be implemented. This has been one of the main challenges of this project.

The rest of this section is organized as the following: first, the GUI (Graphical User Interface) is introduced; then, the structure of all the variables and data is commented; after the organization of the code is presented, and, finally, the integration of the WINNER II channel is explained.

4.2.1 Organization of the GUI

One of the most interesting features of MATLAB App Designer is that it allows us to create tabs. This feature is very useful for guiding the user through the setup and separate the settings from the simulation results. Besides, the aspect of the app is cleaner, and the user interaction is more intuitive than with GUIDE. Figure 4.7 shows the first tab of the simulator.

As we can see, there are five tabs in total:

- **Settings:** This is the first step for running the simulator. Here the setup of the simulation is selected.
- **Layout:** In this tab, the position of the UEs and the gNB is established. Besides, there is a button to generate the channel.
- **BWPs:** This is the tab in which the BWPs are configured and the initial BWP allocation is carried out
- **SNR – Simulation:** This tab corresponds to the Simulation A explained in Section 4.1.3
- **Continuous – Simulation:** This tab corresponds to the Simulation B explained in Section 4.1.3

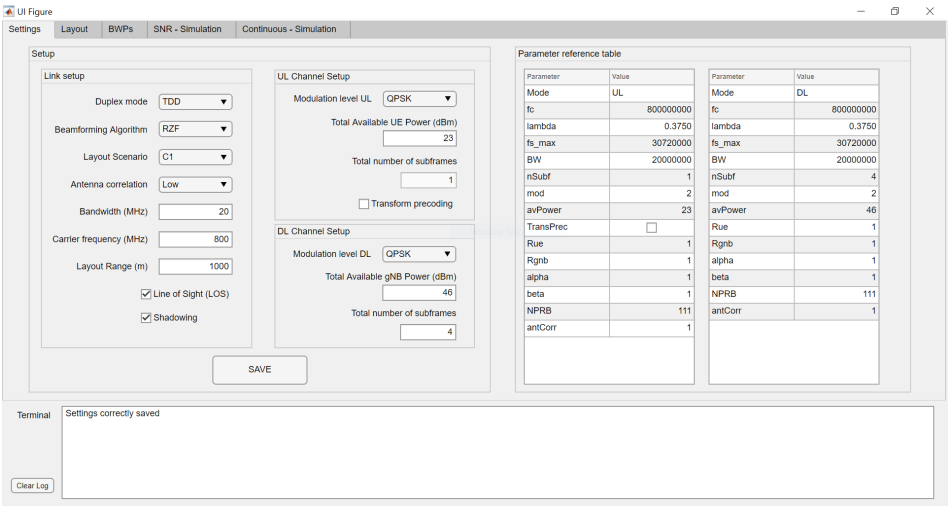

Figure 4.7: First tab of the simulator.

4.2.2 Variable Structure

One of the consequences of the flexibility principle of NR is that there are several different possibilities in the setup of the simulation. Thus, many variables need to be saved and passed to the functions. Besides, a good structure of the data is needed.

For that reason, the best option is to use the structs of MATLAB. The structure arrays of MATLAB (structs) group related data using containers called fields. This type of data makes it quite easy to pass the information to the functions and to organize it.

The main structs of the simulator are gathered up and explained in table 4.1.

4.2.3 Code Structure

When structuring the code, it was essential to facilitate the integration of all the parts of the code and future development of the simulator. For that reason, the code was developed in modules, using MATLAB functions.

This division into modules is based on the blocks shown in Fig. 4.5. In addition to this division, those blocks were also broke down in submodules, which are also MATLAB functions. One example of this subdivision is the block UL Tx. This module was subdivided into all the modules shown in Fig 3.3.

This implementation not only enables further developments of the code but also facilitates the understanding of the code.

4.2.4 Channel Integration

Finally, another of the main challenges of the project was to integrate the WINNER II channel into the simulator.

Struct	Description
UEs	Information about the UEs such as position, number of antennas or identifier
gNB	Information about the gNB position, number of antennas or antenna spacing
BWPs	BWP allocation and information about the BWPs, such as the number of RBs or numerology.
chUL	Parameters of the uplink, such as center frequency, sampling frequency, bandwidth or the modulation
chDL	Parameters of the downlink, such as center frequency, sampling frequency, bandwidth or the modulation
ch_set	Channel model settings, such as the layout scenario
sim_param	Simulation parameters, such as the beamforming algorithm or the SNR range.
results	Results of the simulation, such as the constellations or the BER.

Table 4.1: Data structs in the simulator implementation

As stated before, the channel model that is used was developed by MATLAB and can be downloaded from their website.

This implementation of the WINNER II channel model gives a multidimensional channel matrix H containing time-variant Channel impulse responses between all transmitter and receiver antenna combinations of MIMO system. Besides, it also generates the multipath delays for all the links.

The integration of the WINNER II channel can be divided into three steps: initial setup of the channel, channel update and matrix generation, and channel step.

Initial setup

The first step is to pass the settings fixed by the user in the user interface to the WINNER II channel model. For that purpose, first, the antenna array of each user and base station is configured. Then, the system layout is set: position, LOS/NLOS, link pairing... Finally, the rest of the model parameters are fixed, and one random seed is selected. This random seed is critical because it allows the simulator to use the same environment, i.e., scatters for the three experiments.

Channel update and matrix generation

Once that the channel setup is configured and one simulation is launched, it is time to get a channel realization for each run of the simulator. However, when changing any of the parameters of the initial setup, the channel parameters have

to be updated. It is then essential to keep the same random seed to maintain the same environment.

Finally, a channel realization through a five dimensions matrix is generated. The five dimensions are number or receivers, number of transmitters, number of multipaths, number of samples, and number of users. Jointly to the channel matrix, the multipath delays are also obtained.

Channel step

Lastly, the channel effect has to be applied to the transmitted signals by the users or the base stations.

Equation 4.1 shows the received signal for a UE k.

$$y_k(t) = \sum_{i=1}^{N_{Tx}} \sum_{j=1}^{N_{Rx}} \sum_{n=1}^{N_{Paths}} x(t - \tau_T) \cdot H_k(i, j, n, t) \cdot G_{ant} \cdot \frac{1}{\sqrt{PL_k}} \tag{4.1}$$

$$\tau_T = \tau_s + \tau_p \tag{4.2}$$

Where $x(t)$ is the signal transmitted, H is the channel multi-dimensional matrix, G_{ant} is the antenna gain, PL_k is the corresponding path loss for a given UE, τ_p is the delay due to the distance between the gNB and the UE, and τ_p is the relative delay due to each path, being 0 for the LOS.

Chapter 5

Bandwidth Part Selection Algorithm

Once that the whole simulator was designed and implemented, it was time to develop the Bandwidth Part Selection algorithm. The purpose of this algorithm was to optimize the channel capacity through Bandwidth Part switching. It shall be highlighted that the goal of the algorithm is not to choose from the beginning the best MU-MIMO grouping for each BWP. Instead, the aim is to respond to the time evolution of the environment and change the UEs grouping to keep the initial cell capacity or performance. It should also be clarified that one MU-MIMO group makes use of one BWP with its numerology, so when we refer to an MU-MIMO group or a BWP, we are referring to the same concept.

The first thing that we need to develop the algorithm is finding metrics that are suitable to identify when the performance of the cell is decreasing. The initial guess was to use the estimated SNR and the channel correlation. However, the channel correlation is not a useful metric. The reason is that it allows us to detect when two UEs of the same MU-MIMO grouping are experiencing the same channel. However, this metric can not be used to compare the channel from UEs that are in different BWPs because those channels are never correlated. Thus, we needed to find another metric.

The second candidate for the metric was the Direction of Arrival (DOA). DOA algorithms allow us to find the direction from which the signal is coming. Besides, we can obtain the signal power that is coming from every angle if we use algorithms like Multiple Signal Classification (MUSIC). This signal power profile can be used to identify UEs closely located. The reason is that if two UEs are experiencing the same signal power profile, they are probably being affected by the same scatters, and thus, the channel is correlated, and they can not be in the same MU-MIMO group. Thus, this metric was suitable for the project.

The rest of the chapter is organized as follows: first, the MUSIC Algorithm is introduced, and then, the algorithm operation is described.

5.1 DOA Algorithms: MUSIC

Ralph O. Schmidt defined the term MUltiple SIgnal Classification (MUSIC) [24] as “the experimental and theoretical techniques involved in determining the parameters of multiple wavefronts arriving at an antenna array from measurements

made on the signals received at the array elements. " This algorithm can be used to provide asymptotically unbiased estimates of the number of signals, the directions of arrival (DOA), strengths and cross-correlations among the directional waveforms, polarizations, and strength of noise/interference.

In this project, we want to use the algorithm to estimate the Direction of Arrivals and the strength of the directional waveforms. For that purpose, we used the algorithm developed by Mahmoud Mohanna et al. [25].

The MUSIC algorithm is based on the fact that a received signal in a uniform linear array antenna can be represented with the following mathematical model. In the model that we present here, we consider that there is only one incoming wave.

$$\boldsymbol{a(\theta)} = \begin{bmatrix} 1 \\ e^{j\beta d \sin(\theta)} \\ e^{j2\beta d \sin(\theta)} \\ \vdots \\ e^{j(M-1)\beta d \sin(\theta)} \end{bmatrix} \tag{5.1}$$

Where $a(\theta)$ is the steering vector, $\beta = 2\pi/\lambda$ is the incident wave number and d is the antenna element spacing. Then,

$$\begin{bmatrix} y_1(k) \\ y_2(k) \\ \vdots \\ y_M(k) \end{bmatrix} = \boldsymbol{a}(\theta) \cdot x(k) + \boldsymbol{n}(k) \tag{5.2}$$

Where $x(k)$ is the transmitted signal and $\boldsymbol{n(k)}$ is the noise vector with the noise at each element m.

The MUSIC algorithm is composed of the following steps: Correlation Matrix Calculation, Eigen-decomposition, MUSIC Spectrum Calculations, and Estimation of the largest peaks.

- **Correlation Matrix Calculation**: Given the antenna data, i.e., a matrix X with dimensions MxL where M is the number of antennas and L the number of samples, a correlation matrix MxM is computed with the following formula:

  $$\boldsymbol{R} = \boldsymbol{x} \cdot \boldsymbol{x}^H \tag{5.3}$$

  Where H is Hermitian (i.e. conjugate transpose)

- **Eigen-Decomposition**: The correlation matrix is decomposed into two orthogonal matrices: signal-subspace and noise-subspace. The assumption is that the noise in each channel is highly uncorrelated so that the correlation matrix is diagonal.

The correlation matrix has M eigenvalues associated with M eigenvectors. Thus, we can decompose the correlation matrix, $\boldsymbol{R}$, like shows Equation 5.4.

$$\boldsymbol{R} = \boldsymbol{V}\boldsymbol{\Lambda}\boldsymbol{V}^{-1} \tag{5.4}$$

If we sort the eigenvalues from largest to smallest, we can divide the eigenvector matrix, $\boldsymbol{V}$, into two subspaces $[\boldsymbol{V_N} \quad \boldsymbol{V_S}]$. The first subspace, $\boldsymbol{V_N}$, is the noise subspace, and it has M-1 eigenvectors associated with the noise. The second subspace, $\boldsymbol{V_S}$, is the signal subspace, and it only has one eigenvector associated with the incoming signal.

- **MUSIC Spectrum Calculations**: The noise subspace eigenvectors are orthogonal to the array steering vectors, $\boldsymbol{a(\theta)}$, at the angles of arrival. For that reason, it can be shown that $\boldsymbol{a(\theta)}^H \boldsymbol{V_N} \boldsymbol{V_N}^H \boldsymbol{a(\theta)} = 0$ for every arrival angle [25]. Then, the MUSIC pseudo spectrum is given as

$$\boldsymbol{P}(\theta) = \mathrm{PMU}(\theta) = \frac{\boldsymbol{a(\theta)}^H \boldsymbol{a(\theta)}^H}{\boldsymbol{a(\theta)}^H \boldsymbol{V_N} \boldsymbol{V_N}^H \boldsymbol{a(\theta)}} \tag{5.5}$$

- **Estimation of the largest peaks**: Finally, the argument of the peaks of the abovementioned pseudo spectrum gives the angle of arrival

5.2 Description of the algorithm

The BWP selection algorithm can be run when a UL subframe arrives at the gNB. As a complex modulation such as OFDMA is used, the signals received from each user are split before computing the DOA. This way, the assumption of only one incoming signal used in the previous section is still valid. For that reason, we need to process the received signal before obtaining the DOA and calling the BWP selection algorithm. This pre-processing is shown in Fig. 5.1.

First, the channel estimation is done so that the received signal can be equalized. Once equalized, the subframe can be extracted, and the symbols from each user split in separated streams. Then, with each independent symbol stream from each user, new subframes are created, and the channel effect is applied again (inverse process to the equalization). The reason for applying the channel effect again is that it carries the information of the angle of arrival. After, the subframe grid is OFDM-modulated to obtain time-domain signals.

As a result, we get one time-domain signal per user. With these signals, we call the MUSIC algorithm (once per user), and we obtain the power profile (MUSIC pseudo-spectrum) for each user. This power profile is the metric that is used by the actual selection algorithm, and it is given by the channel estimation function.

Then, the actual BWP selection algorithm can be called (see Fig. 5.2). The algorithm is run for each user. The first step is to compare the estimated SNR with a given threshold. If the SNR is above the threshold for all the UEs, the BWPs are kept, and the algorithm execution is finished.

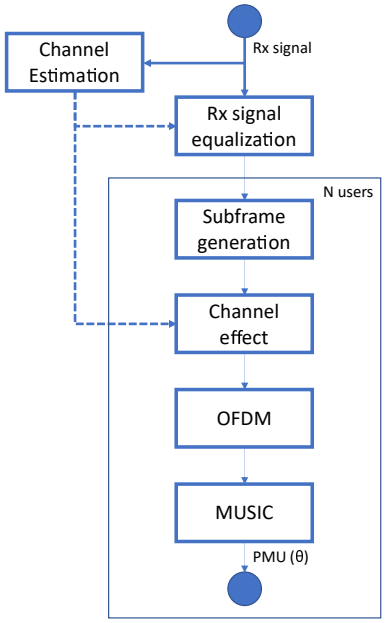

Figure 5.1: DOA pre-processing flow.

Otherwise, a list with the UEs whose SNR was below the threshold is created. For each UE in the list, the channel correlation is computed from the channel estimations with each other UE inside the same MU-MIMO group. Those correlations are compared with another threshold. If all the correlations are below the threshold, i.e., the channels are not too similar, the UE is withdrawn from the list.

If the list is empty, the BWPs are kept, and the algorithm execution is finished. Finally, the UEs that are still in the list are reallocated to a new MU-MIMO grouping (BWP) following this expression.

$$\mathrm{BWP}|_{\mathrm{UE}_n} = \underset{\mathrm{BWP}_i}{\operatorname{argmax}} \left(\sum_{\mathrm{UE}_j \in \mathrm{BWP}_i} \left\| \frac{\boldsymbol{P_n}(\boldsymbol{\theta})}{\max\left(\boldsymbol{P_n}(\boldsymbol{\theta})\right)} - \frac{\boldsymbol{P_j}(\boldsymbol{\theta})}{\max\left(\boldsymbol{P_j}(\boldsymbol{\theta})\right)} \right\| \right) \tag{5.6}$$

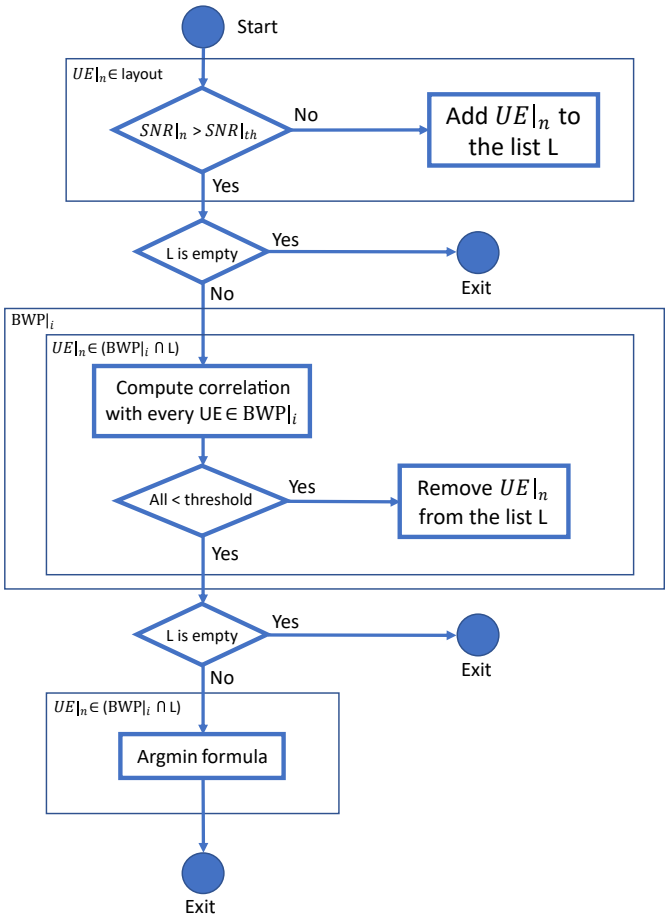

Figure 5.2: BWP-selection algorithm flow.

Chapter 6
Results

This chapter presents the results obtained for the two simulations presented in Section 4.1.3 for different scenarios. The goal is to validate not only the BWP-selection algorithm but also the WINNER 2 channel that is used.

For that purpose, 3 different scenarios have been tested, which are summarized in Table 6.1.

ID	N users	Initial Allocation	Description
1	2	BWP1: UE1, UE2 BWP2: -	UE1 and UE2 initially 200m separated. UE1 gets close to UE2
2	3	BWP1: UE1, UE2 BWP2: UE3	UE1 and UE3 initially close. UE1 gets close to UE2 while UE3 stays in the same place
3	3	BWP1: UE1, UE2 BWP2: UE3	Similar to the second scenario but with a shorter distance between UE1 and UE3, and UE2

Table 6.1: Simulation scenarios summary table

6.1 Scenario 1

The first scenario consists of two users that are separated 200m from each other at the beginning. Then, User 1 starts to move in the direction of the other one until the distance between them is 1m (final position).

Each of the two users only has one antenna, and the base station has eight antennas. Both the uplink and the downlink use QPSK modulation. The total available power for the UE is 23 dBm and 46 dBm for the base station. The beamforming technique used for the downlink is *Regularized Zero-Forcing*.

The channel is modeled with WINNER II, and there is Line of Sight (LOS) and shadowing. The WINNER II scenario is C1, which corresponds to a suburban environment.

The bandwidth available for the cell is 20 MHz, and the carrier frequency, 800 MHz.

The initial layout and the final layout are shown in Fig. 6.1 and Fig. 6.2, respectively.

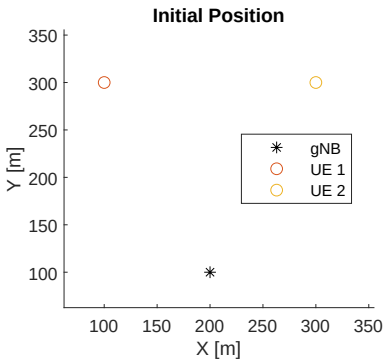

Figure 6.1: Initial position

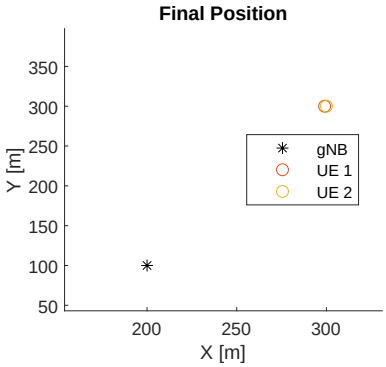

Figure 6.2: Final position

Two BWPs are configured for this simulation, both of them composed of 40 resource blocks and with a numerology of 15 kHz. Both UEs are allocated with the same BWP, i.e., they belong to the same MU-MIMO group. The BWP allocation is represented in Fig. 6.3. This figure shows the two BWP with different colors. The scale relates the colors with the BWP ID: the green represents BWP1, and the yellow represents BWP2. The area in dark blue is not allocated to any BWP. Note that the x-axis represents the number of resource blocks for the given cell bandwidth.

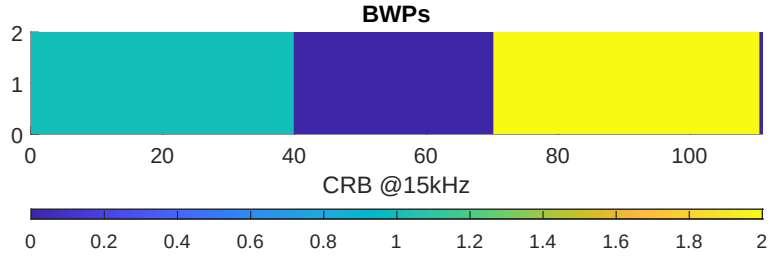

Figure 6.3: Configured BWPs.

Figure. 6.4 shows the received signal at the gNB when the optimization algorithm is activated, and the UEs are allocated with different BWP. We can see the two BWP allocations in the plot and that there is no overlapping between them.

6.1.1 Simulation A

As explained in Section 4.1.3, the first simulation shows the performance of the cell for different SNRs. The results are shown in Figure 6.5. In this figure, three

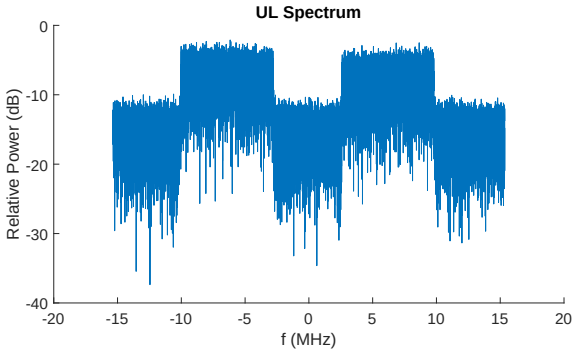

Figure 6.4: Simuation 1: UL Rx Spectrum.

lines are shown. The first one (*static*) corresponds to the performance in the initial situation. As both UEs are far from each other, they experience different channels, and the beamforming can be carried out. Thus, we get the expected BER curve. However, the second curve (*Same BWP*) corresponds to the case in which the two UEs are very close (1m far), so they experience the same channel. As a consequence, the beamforming performance is very poor, and the BER does not decrease as expected with the SNR.

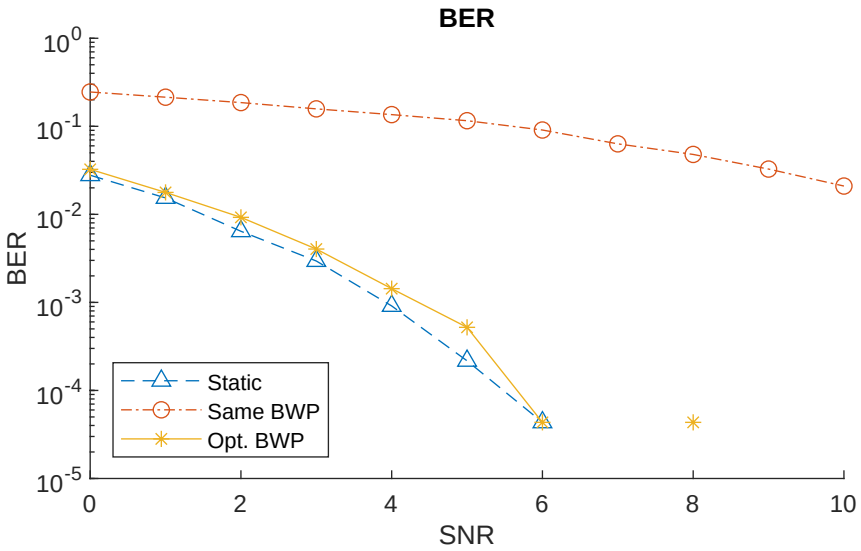

Figure 6.5: Simuation 1A: BER Performance.

Finally, the curve (*Opt. BWP*) shows the performance when the optimization algorithm is run for the same UEs position as in *Same BWP*. As we can see, there is an improvement in the performance, and it gets close to *static* curve. Thus, the user would not experience any degradation in the service when moving in the layout.

For the sake of making a fair comparison between the curves, the same noise has been added to the three experiments. In other words, the noise power was computed for each SNR for the first curve, and then the same noise power was applied to the other two curves.

6.1.2 Simulation B

The second simulation shows the temporal evolution of the bit error rate and the BWP switching. The path between the initial position and the final position is divided, in this case, into 20 snapshots. Then, the SNR is fixed for all these snapshots to 4 dB. The performance in these snapshots, or sample points, is shown in Fig. 6.6. In addition, the MU-MIMO grouping, i.e., the BWPs, are shown in Fig. 6.7.

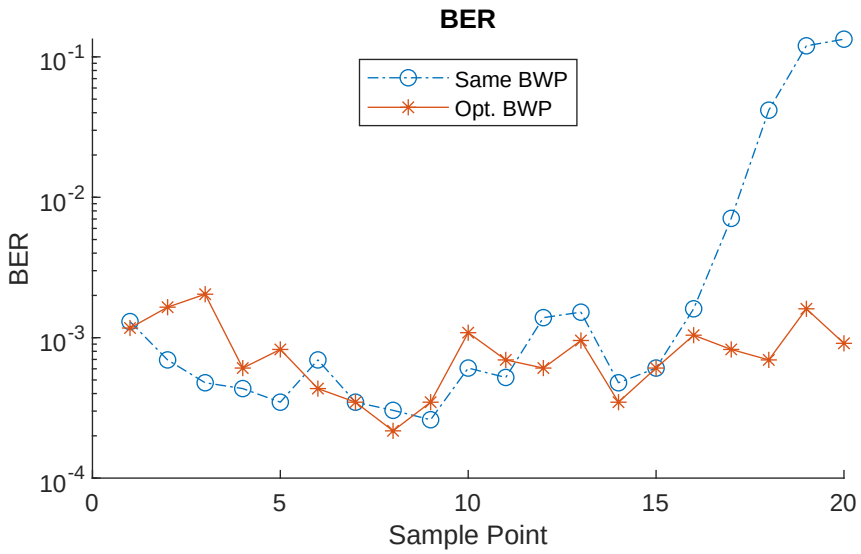

Figure 6.6: Simuation 1B: BER Performance.

In this simulation, there are two curves represented. The first one, Same BWP, shows the performance when the BWP-selection algorithm is not activated. The second one, Opt. BWP, corresponds to the case in which the algorithm is activated.

We can see in the BER figure that the performance is improved when the algorithm is used. In the last sample points, the two UEs are two close, so the algorithm separates them into two different MU-MIMO groups. As a consequence, the BER remains flat, instead of degenerating as in the Same BWP curve. However, we can see as well that in the first points, the algorithm also separates the two UEs into two BWP. Nevertheless, this effect is not translated into a great degeneration of the performance.

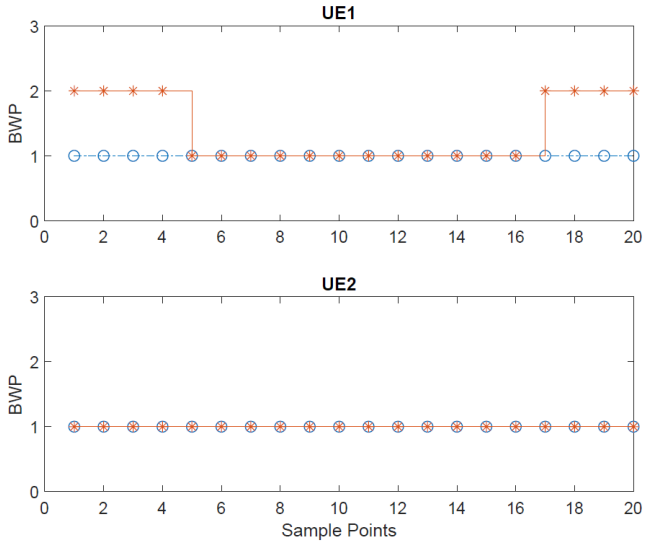

Figure 6.7: Simulation 1B: UEs BWP switching.

6.2 Scenario 2

The second scenario is very similar to the previous one, but a new UE is added to the simulation. The rest of the parameters, such as the center frequency or the modulations, are kept.

The BWPs configured in Scenario 1 are also kept, with the 15 kHz subcarrier spacing and the size of 40 Resource Blocks (RBs).

The third UE is located close to the first one (see Fig. 6.8) and has an initial allocation of BWP2. Note that in Fig. 6.9 UE1 and UE 2 are so close that they can almost not be identified.

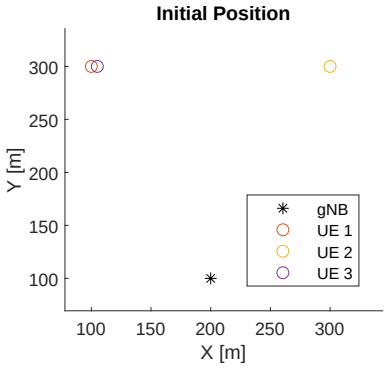

Figure 6.8: Initial position

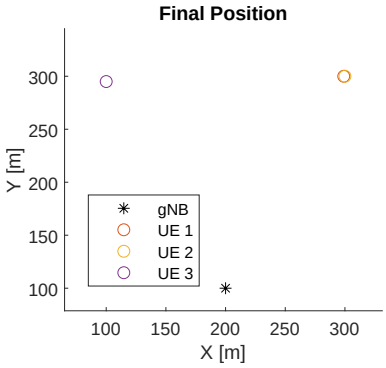

Figure 6.9: Final position

6.2.1 Simulation A

The first simulation shows the SNR-performance of the BWP-selection algorithm again. As we can see in Fig. 6.10, the *Opt. BWP* curve is really close to the *Static* curve, while the *Same BWP* curve has a worse performance than the others. In this case, we have computed the performance using two different beamforming algorithms, Regularized ZE and MRT.

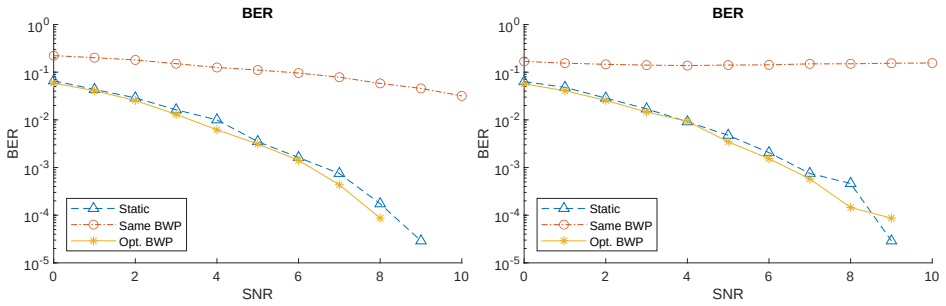

(a) Regularized ZF (RZF) **(b)** Maximum Ratio Transmission (MRT)

Figure 6.10: Simuation 2A: BER Performance.

The figure shows that the performance when using the MRT weighting is notably worse for the *Same BWP* curve. The reason is that this technique is more sensitive to inter-user interference, which is higher in the *Same BWP* case.

6.2.2 Simulation B

In this scenario, Simulation B gives us more information about the algorithm than Simulation A. In this case, the BWPs are always scheduled with at least one UE. This means that the number of UEs per BWP is always 1 or 2. As the two BWP are similar, the only difference is which UE is in which BWP. In other words, global performance is not affected by the number of UEs per BWP (because it is constant) but for the sorting of those UEs. The SNR was fixed to 6 dB in this simulation. We show again the performance for MRT and RZF beamforming.

Then, we can see that, in this case, the performance of the optimization algorithm is always better even though UE2 changes the BWP allocation for the first ten sampling points (see Fig. 6.11 and Fig. 6.12). Besides, we can see that when the BWP-selection algorithm is not used, i.e., the *Same BWP* curve, the performance gets worse in a previous sample point in the MRT plot than in the RZF plot. In essence, this means that the users have to get closer when using the RZF beamforming to get the same degradation than when using the MRT technique.

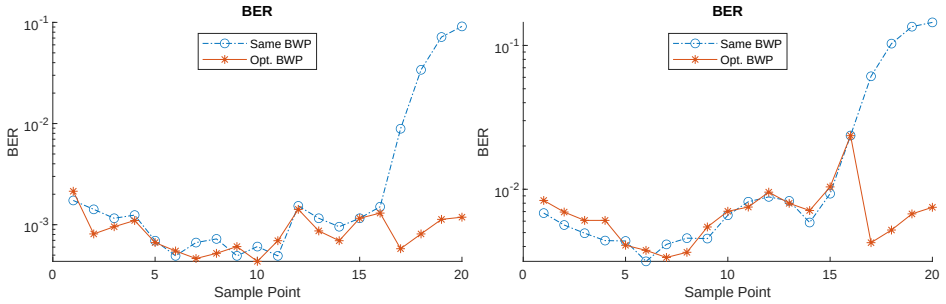

(a) Regularized ZF (RZF) **(b)** Maximum Ratio Transmission (MRT)

Figure 6.11: Simuation 2B: BER Performance.

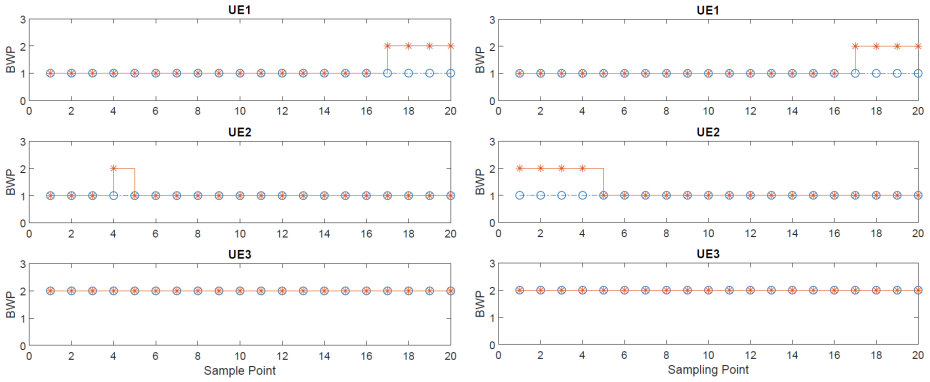

(a) Regularized ZF (RZF) **(b)** Maximum Ratio Transmission (MRT)

Figure 6.12: Simulation 2B: UEs BWP switching

6.3 Scenario 3

Then, a third scenario was tested with a shorter distance between the UEs. The scenario has the same characteristics as Scenario 2, but the distance between UE1 and UE3, and UE3 was 100m.

The goal of this scenario was to study the impact of other configuration parameters in the performance. For that purpose, only Simulation A was used.

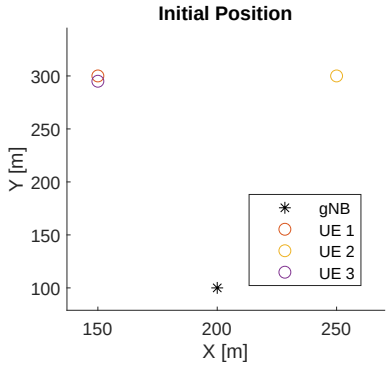

Figure 6.13: Initial position

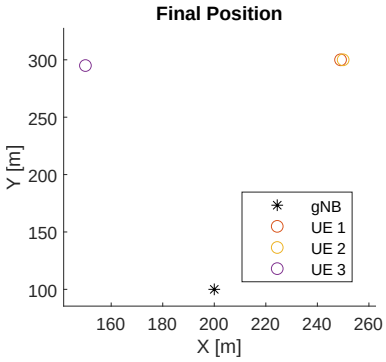

Figure 6.14: Final position

All the configuration parameters except the layout, shown in Fig. 6.13 and Fig. 6.14, also apply for the default case of this scenario. Then, some parameters are changed one by one and compared with that default case, as explained below.

6.3.1 Impact of the modulation

First, we show a comparison between a default case, QPSK, and one simulation in which the uplink and downlink modulation was 16-QAM.

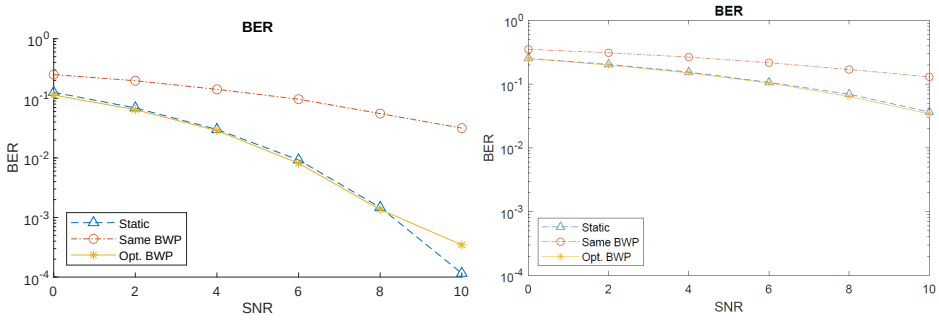

(a) QPSK **(b)** 16-QAM

Figure 6.15: Simulation 3: Impact of the modulation BER Performance

The figure shows that the modulation has a high impact on the SNR to all the curves. What we can see is that the curves on the left and the right plots are shifted around 8 dB. However, the benefit of using higher modulations is that the overall bit rate is increased.

6.3.2 Impact of the numerology

Finally, we present a comparison of the performance of two numerologies. The default simulation used a subcarrier spacing of 15 kHz, and the new simulation used a subcarrier spacing of 30 kHz. However, the allocation bandwidth remained constant, which means that fewer resource blocks were allocated to the second case.

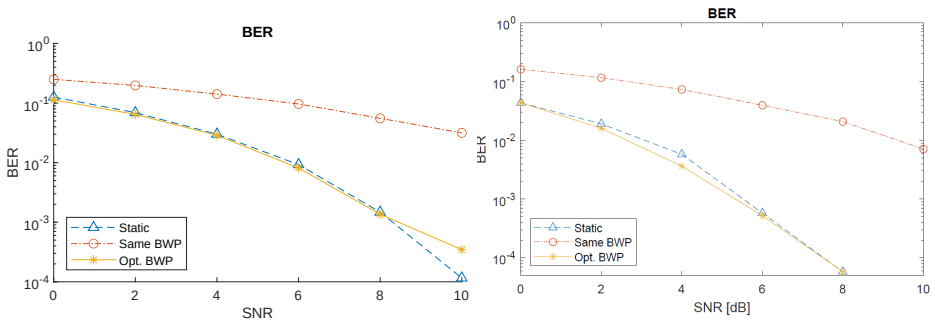

(a) 15 kHz subcarrier spacing **(b)** 30 kHz subcarrier spacing

Figure 6.16: Simulation 3: Impact of the numerology

A change in the subcarrier spacing while keeping the same allocated bandwidth implies that the number of resource blocks and thus, resource elements, is reduced. However, if a higher subcarrier spacing is used, the resistance to frequency errors and phase noise is increased. In Fig 6.16 we can see that there is a gain of around 2 dB.

Chapter 7

Conclusions and Future Work

7.1 Conclusions

We started this Master Thesis presenting the novelties of the New Radio standardized for 5G and the need for flexibility in the technical requirements for fulfilling the use cases. One of the new characteristics was the inclusion of Bandwith Parts (BWPs). Then, we showed the need for a detailed analysis of the impact of BWPs in the MU-MIMO grouping and beamforming.

For that reason, we designed and implemented one simulator in MATLAB following the Specifications of the 3GPP and developed an optimizing algorithm for taking advantage of the BWPs without losing capacity because of the MU-MIMO degradation.

When designing the simulator, we realized that the channel model selection was critical for obtaining realistic results, and the importance of the spatial consistency was highlighted. We studied the state of the art of modern channel models that could be used with beamforming, and we selected the WINNER 2 implementation for MATLAB.

Then, a Bandwidth-Part selection algorithm was developed, making use of the Direction of Arrival (DOA) as a metric for optimizing the BWP selection. To that end, a DOA estimation algorithm had to be implemented, and the MUSIC algorithm was found as appropriate for that function.

Once the simulator and the BWP-selection algorithm were designed and implemented, it was time for testing them. To that end, some scenarios were defined with different users moving in a simulated environment.

The results show that the WINNER II channel can emulate the degradation of the beamforming when two users in the same MU-MIMO group are close to each other. Besides, Chapter 6 also proved that the optimizing algorithm could maintain the same BER performance for all the user position without a dependency on their relative position (for the scenarios tested).

Thus, we can consider that the simulator is validated and meets the 3GPP 5G/NR requirements. This simulator can help to research and optimize new techniques to improve the performance of NR. Besides, we can also state that the developed BWP-selection algorithm improves the BER performance.

7.2 Future Work

The main task during this thesis was to develop the NR simulator suitable for testing the BWPs. For that reason, there was no time for developing advanced algorithms or testing with all the parameter configurations available in 5G/NR.

As a consequence, there are two main areas related to this thesis where the work can be expanded: new parameter configurations and new algorithms.

First, the simulator already implements some support to multiple layers per user. However, it is not entirely integrated with the channel sounding and the presented BWP-selection algorithm. Multiple-layers support is one feature extensively used in NR, so it should be included and tested in this simulator. Then, Winner II was an appropriate channel for this first version of the simulator, but more advanced channel models can be added. For instance, QuaDRiGa [18] is an up-and-coming free-access channel model that can be integrated into the simulator. This simulator was included in the 3GPP Recommendation 38.901 [4] when they mentioned other works on channel modeling.

Secondly, more advanced algorithms making use of other types of metrics can also be used. In this project, we already used the channel correlation and the DOA. However, the use of these metrics can still be optimized using new strategies like, for instance, machine learning. In addition, new metrics can be found to improve the performance of the algorithm based on parameters obtained from the channel states and control signaling.

Finally, the results of this project have been obtained with non-overlapping BWPs. However, overlapping BWPs are also allowed in NR, so the impact of these BWPs in the optimization algorithms should also be analyzed.

References

[1] 3GPP, "Release description; Release 15," TR 21.915, Sep. 2019.

[2] ——, "5G; NR; Physical channels and modulation," TS 38.211, Dec. 2019.

[3] F. Abinader, A. Marcano, K. Schober, R. Nurminen, T. Henttonen, H. Onozawa, and E. Virtej, "Impact of Bandwidth Part (BWP) Switching on 5G NR System Performance," in *2019 IEEE 2nd 5G World Forum (5GWF)*, Sep. 2019, pp. 161–166.

[4] 3GPP, "5G; Study on channel model for frequencies from 0.5 to 100 GHz," Technical Report 38.901, Jul. 2018.

[5] S. Ju and T. S. Rappaport, "Simulating Motion - Incorporating Spatial Consistency into NYUSIM Channel Model," in *2018 IEEE 88th Vehicular Technology Conference (VTC-Fall)*, Aug. 2018, pp. 1–6.

[6] F. Ademaj, S. Schwarz, T. Berisha, and M. Rupp, "A Spatial Consistency Model for Geometry-Based Stochastic Channels," *IEEE Access*, vol. 7, pp. 183 414–183 427, 2019.

[7] Ericsson, "5G wireless access: an overview," White Paper, Apr. 2020.

[8] E. Dahlman, S. Parkvall, and J. Sköld, *5G NR: The next generation wireless access technology*, 1st ed. Academic Press, 2018.

[9] NGMN Alliance, "5G White Paper," White Paper, Feb. 2015.

[10] 3GPP, "5G; NR; User Equipment (UE) radio transmission and reception; Part 1: Range 1 Standalone," TS 38.101-1, Mar. 2020.

[11] 3GPP, "5G; NR; User Equipment (UE) radio transmission and reception; Part 2: Range 2 Standalone," TS 38.101-2, Mar. 2020.

[12] The MathWorks, "Understanding the 5G NR Standard," accessed: 28/5/2020. [Online]. Available: https://se.mathworks.com/videos/series/understanding-the-5g-nr-standard.html

[13] S. DeTomasi, "Understanding 5G New Radio Bandwidth Parts," Nov. 2018, accessed: 18/5/2020. [Online]. Available: https://blogs.keysight.com/blogs/inds.entry.html/2018/10/31/understanding_5gnew-iYIV.html

[14] A. Paulraj, A. P. Rohit, R. Nabar, and D. Gore, *Introduction to Space-Time Wireless Communications*. Cambridge University Press, May 2003.

[15] P. Almers, E. Bonek, A. Burr, N. Czink, M. Debbah, V. Degli-Esposti, H. Hofstetter, P. Kyösti, D. Laurenson, G. Matz, A. F. Molisch, C. Oestges, and H. Özcelik, "Survey of Channel and Radio Propagation Models for Wireless MIMO Systems," *J Wireless Com Network*, vol. 2007, no. 1, pp. 1–19, Dec. 2007. [Online]. Available: https://jwcn-eurasipjournals.springeropen.com/articles/10.1155/2007/19070

[16] 3GPP, "Universal Mobile Telecommunications System (UMTS); Spatial channel model for Multiple Input Multiple Output (MIMO) simulations," Technical Report 25.996, Jul. 2018.

[17] P. Kyösti, J. Meinilä, L. Hentilä, X. Zhao, and T. Jämsä, "WINNER II Channel Models," IST, Technical Report IST-4-027756, Sep. 2007.

[18] S. Jaeckel, "Quasi-deterministic channel modeling and experimental validation in cooperative and massive MIMO deployment topologies," Ph.D. dissertation, TU Ilmenau, Ilmenau, Aug. 2017.

[19] L. Liu, J. Poutanen, F. Quitin, K. Haneda, F. Tufvesson, P. Doncker, P. Vainikainen, and C. Oestges, "The COST 2100 MIMO channel model," *IEEE Wireless Communications*, vol. 19, pp. 92–99, Dec. 2012.

[20] S. Andersson and W. Tidelund, "Adaptive Beamforming for Next Generation Cellular System," LTH, Lund University, Lund, Master Thesis, Sep. 2016.

[21] C. K. R. Veluru and A. C. Rohan, "Intelligent Beam Weight Computation for Massive Beamforming," Blekinge Institute of Technology, Karlskrona, Master Thesis, Jun. 2017.

[22] A. Hatahet and A. Jain, "Beamforming in LTE FDD for Multiple Antenna Systems," LTH, Lund University, Lund, Master Thesis, May 2018.

[23] The MathWorks, "Develop Apps Using App Designer," accessed: 01/06/2020. [Online]. Available: https://se.mathworks.com/help/matlab/app-designer.html

[24] R. Schmidt, "Multiple emitter location and signal parameter estimation," *IEEE Transactions on Antennas and Propagation*, vol. 34, no. 3, pp. 276–280, Mar. 1986.

[25] M. Mohanna, M. L. Rabeh, E. M. Zieur, and S. Hekala, "Optimization of MUSIC algorithm for angle of arrival estimation in wireless communications," *NRIAG Journal of Astronomy and Geophysics*, vol. 2, no. 1, pp. 116–124, Jun. 2013. [Online]. Available: http://www.sciencedirect.com/science/article/pii/S209099771300031X

List of acronyms

AMPS	Advanced Mobile Phone System
AR	Augmented Reality
BCCH	Broadcast Control Channel
BCH	Broadcast Channel
BER	Bit Error Rate
BPSK	Binary Phase-Shift Keying
BWP	Bandwidth Part
CCCH	Common Control Channel
CDMA	Code Division Multiple Access
CRC	Cyclic Redundancy Check
CSI	Channel Status Information
DCCH	Dedicated Control Channel
DFT	Discrete Fourier Transform
DL	Downlink
DOA	Direction of Arrival
DTCH	Dedicated Traffic Channel
EPC	Evolved Packet Core
FDD	Frequency-Division Duplexing
GSM	Global System for Mobile communications
GUI	Graphical User Interface
HSPA	High-Speed Packet Access
IEEE	Institute of Electrical and Electronics Engineers
ITU	International Telecommunication Union
LOS	Line Of Sight
LSP	Large Scale Parameter
LTE	Long-Term Evolution
MAC	Medium Access Control
eMBB	enhanced Mobile Broadband
MIMO	Multiple-Input Multiple-Output
MMSE	Minimum Mean Square Error
MRT	Maximum Ratio Transmission
mMTC	massive Machine-Type Communications
MU-MIMO	Multi-User MIMO

MUSIC	Multiple Signal Classification
gNB	gNodeB
NGMN	Next Generation Mobile Networks
NLOS	Non Line of Sight
NMT	Nordisk MobilTelefoni
NR	New Radio
NSA	Non-Standalone
OFDM	Orthogonal Frequency Division Multiplexing
OFDMA	Orthogonal Frequency Division Multiplexing Access
PAPR	Peak-to-Average Power Ratio
PBCH	Physical Broadcast Channel
PCCH	Paging Control Channel
PCH	Paging Channel
PDCCH	Physical Downlink Control Channel
PDSCH	Physical Downlink Shared Channel
PRACH	Physical Random-Access Channel
PUCCH	Physical Uplink Control Channel
PUSCH	Physical Uplink Shared Channel
QAM	Quadrature Amplitude Modulation
QPSK	Quadrature Phase-Shift Keying
RACH	Random-Access Channel
RB	Resource Block
RLC	Radio Link Control
SA	StandAlone
SCM	Spatial Channel Model
SINR	Signal-to-Interference-Plus-Noise Ratio
SNR	Signal-to-Noise Ratio
SRS	Sounding Reference Signal
SS	Synchronization Signal
SSP	Small-Scale Parameter
TDD	Time-Division Duplexing
UE	User Equipment
UL	Uplink
UMTS	Universal Mobile Telecommunications System
URLLC	Ultra-Reliable Low Latency Communications
VR	Virtual Reality
ZF	Zero-Forcing